

Electronic Supplementary Information:

Differences in actinide metal-ligand orbital interactions: comparison of U(IV) and Pu(IV) β -ketoiminate N,O donor complexes

David D. Schnaars, Enrique R. Batista,* Andrew J. Gaunt,* Trevor W. Hayton,* Iain May, Sean D. Reilly, Brian L. Scott and Guang Wu

Practicalities of Transuranic Research and Safety Considerations. Work with plutonium of weapons-grade isotopic composition (primarily ^{239}Pu) was conducted in a radiological facility approved to contain high specific activity α -emitting radionuclides, with appropriate controls for the safe handling and manipulation of radioactive materials. The hazards posed by the radionuclide ^{239}Pu imposes a number of controls and work restrictions necessary to gain safety approvals at Los Alamos National Laboratory. As a consequence, we are unable to acquire elemental analyses on transuranic solids (no in-house capability exists; no user facility can readily or safely accept dispersible transuranic solids). Similarly, the balance of contamination control techniques with the sample configurations designed to protect air-sensitive samples (often samples must be exposed to air to allow swipe tests to detect loose contamination before transportation to spectrometer to comply with local safety rules) currently prevent us from acquiring IR data on air-sensitive transuranic compounds.

Experimental Details:

Synthesis of 1: To a suspension of UCl_4 (131.8 mg, 0.347 mmol) in Et_2O (3 cm^3) was added two equiv of $\text{H}^{\text{Ar}}\text{acnac}$ (285.7 mg, 0.694 mmol) and $\text{Na}[\text{N}(\text{SiMe}_3)_2]$ (127.6 mg, 0.696 mmol) resulting in a deep red solution. After stirring for 25 h, the volatiles were removed in vacuo and the resulting solid was washed with hexanes ($2 \times 5 \text{ cm}^3$) before dissolution in dichloromethane (8 cm^3), to give a deep red cloudy solution, which was filtered though Celite and concentrated in vacuo (3 cm^3). Storage at -25 °C for 48 h resulted in the deposition of a dark red block crystals. (77.9 mg, 20% yield). Subsequent concentration of the mother liquor, layering with hexanes, and storage at -25 °C produced additional crystals increasing the total yield (189.6 mg, 48% yield).

Anal. Calcd for $\text{UCl}_2\text{O}_2\text{N}_2\text{C}_{58}\text{H}_{64}$: C, 61.64; H, 5.71; N, 2.48. *Found:* C, 61.34; H 5.35; N, 2.79. $^1\text{H NMR}$ (C_6D_6 , 25 °C, 500MHz): δ 51.13 (br s, 2H, N-aryl para CH), 34.64 (br s, 4H, ortho CH), 16.01 (s, 2H, para CH), 14.94 (br s, 4H, meta CH), 10.54 (br s, 4H, ortho CH), 7.09 (br s, 2H, para CH), 5.72 (br s, 4H, meta CH), -1.22 (br s, 2H, γ -CH), -6.18 (br s, 36H, CMe_3), -50.58 (s, 4H, N-aryl ortho CH). $^1\text{H NMR}$ ($\text{C}_6\text{D}_6 + 1$ equiv THF, 25 °C, 500MHz): δ 35.75 (br s, 4H, ortho CH), 16.12 (s, 2H, para CH), 15.15 (s, 4H, meta CH), 8.62 (br s, 4H, ortho CH), 6.76 (br s, 2H, para CH), 5.20 (br s, 4H, meta CH), -0.50 (br s, 2H, γ -CH), -5.55 (br s, 36H, CMe_3), -49.38 (s, 4H, N-aryl ortho CH). ^1IR (KBr pellet, cm^{-1}): 3233(br w), 3084(w), 3056(w), 3032(w), 3027(w), 2958(s), 2950(sh s), 2924(sh w), 2908(sh w), 2901(w), 2876(sh w), 2866(w), 2360(w), 2338(w), 1593(sh s), 1586(s), 1564(vs), 1542(sh s), 1533(sh s), 1519(m), 1515(m), 1495(sh vs), 1486(sh vs), 1477(vs), 1467(vs), 1460(sh vs), 1450(s), 1439(vs), 1420(sh s), 1392(m), 1362(vs), 1354(sh s), 1333(sh m), 1318(sh m), 1292(vs), 1282(sh s), 1272(sh m), 1258(sh s), 1247(s), 1203(m), 1182(m), 1157(w), 1141(sh w), 1132(m), 1120(m), 1101(m), 1092(m), 1072(s), 1065(s), 1037(w), 1024(s), 1007(w), 999(m), 985(m), 968(w), 931(w), 923(m), 900(m), 888(m), 870(m), 849(w),

841(*w*), 831(*sh w*), 819(*w*), 810(*w*), 778(*sh m*), 771(*s*), 763(*s*), 746(*sh w*), 732(*w*), 710(*s*), 695(*s*), 677(*m*), 667(*m*), 661(*m*), 655(*sh w*), 644(*w*), 637(*w*), 630(*w*), 616(*w*), 603(*w*), 599(*w*), 597(*sh w*), 580(*m*), 565(*m*), 556(*w*), 546(*w*), 5333(*w*), 524(*w*), 519(*w*), 502(*m*), 493(*m*), 485(*w*), 481(*w*), 472(*w*), 469(*sh w*), 459(*w*), 450(*w*), 448(*sh w*), 438(*w*), 428(*w*), 418(*w*), 401(*w*). UV/vis/nIR: (*in CH₂Cl₂, 0.00432 M*) (nm (ϵ)); 718(30), 814(898), 950(23), 1034(20), 1066(27), 1140(12), 1180(14).

Synthesis of 2: Method A: To a cherry red Et₂O solution (5 cm³) of UI₄(OEt₂)₂ (312.2 mg, 0.349 mmol) was added an orange Et₂O solution (3 cm³) containing two equiv Na^{Ar}acnac, produced *in situ* using an equimolar ratio of H^{Ar}acnac (287.9 mg, 0.699 mmol) and Na[N(SiMe₃)₂] (129.2 mg, 0.704 mmol). This resulted in the immediate formation of a green precipitate. The solution was stirred for 20 h producing a pale orange solution containing a green precipitate and a white solid (presumably NaI). The supernatant was decanted off and the solid was washed with Et₂O (2 × 4 cm³) before dissolution of the green solid in CH₂Cl₂ (~40 cm³) to produce a deeply coloured dichroic green/red solution. The solution was filtered through a Celite to remove the white solid, then concentrated in vacuo (10 cm³) and layered with Et₂O. Storage at -25 °C for 72 hours resulted in the deposition of a dark forest green crystalline material (309.5 mg, 67% yield).

Method B: To a cherry red toluene solution (2 mL) of UI₄(OEt₂)₂ (303.9 mg, 0.340 mmol) was added H^{Ar}acnac (279.9 mg, 0.680 mmol) and NEt₃ (100 μL, 0.717 mmol) resulting in the immediate formation of a forest green solution and a green precipitate. After 30 minutes, the volatiles were removed in vacuo and CH₂Cl₂ (25 mL) was added to the solid forming a deeply coloured dichroic green/red solution. The solution was filtered through a Celite column supported on glass wool (0.5 cm × 2 cm) and concentrated in vacuo until crystals began to form. Storage at -25 °C for 4 days resulted in the deposition of a dark forest green crystalline material. The crystalline material was washed with THF (8 mL) and dried in vacuo (286.4 mg, 64% yield).

Anal. Calcd for UI₂O₂N₂C₅₈H₆₄: C, 53.06; H, 4.91; N, 2.13. Found: C, 53.06; H, 4.78; N, 2.13. ¹H NMR (CD₂Cl₂, 25 °C, 500MHz): δ 62.32 (*s*, 2H, *N*-aryl *para* CH), 44.39 (*s*, 4H, *ortho* CH), 19.12 (*s*, 2H, *para* CH), 17.86 (*s*, 4H, *meta* CH), 9.82 (*s*, 4H, *ortho* CH), 7.42 (*s*, 2H, *para* CH), 5.41 (*s*, 4H, *meta* CH), -1.10 (*br s*, CMe₃ of *cis* isomer), -2.88 (*s*, 2H, γ -CH), -3.84 (*br s*, CMe₃ of *cis* isomer), -7.76 (*s*, 36H, CMe₃), -65.02 (*s*, 4H, *N*-aryl *ortho* CH). IR (KBr pellet, cm⁻¹): 3083(*w*), 3060(*w*), 3031(*w*), 2959(*s*), 2930(*sh w*), 2903(*w*), 2865(*w*), 1589(*s*), 1563(*s*), 1493(*sh s*), 1479(*sh vs*), 1470(*vs*), 1454(*sh vs*), 1439(*vs*), 1394(*m*), 1363(*s*), 1316(*sh m*), 1293(*s*), 1247(*m*), 1240(*sh m*), 1206(*w*), 1182(*w*), 1160(*w*), 1133(*w*), 1116(*w*), 1106(*w*), 1077(*m*), 1063(*s*), 1025(*m*), 1000(*w*), 985(*w*), 974(*sh w*), 925(*w*), 923(*sh w*), 901(*m*), 889(*m*), 874(*w*), 843(*w*), 814(*w*), 768(*m*), 731(*w*), 709(*s*), 697(*s*), 688(*s*), 662(*w*), 637(*sh w*), 617(*w*), 600(*w*), 581(*m*), 567(*w*), 547(*w*), 542(*sh w*), 528(*w*), 501(*w*), 494(*sh w*), 483(*sh w*), 452(*w*), 445(*w*), 437(*w*), 417(*w*). UV/vis/nIR: (*in CH₂Cl₂, 0.00439 M*) (nm (ϵ)); 814(53), 894(41), 948(30), 1024(19), 1068(21), 1078(20), 1140(20), 1192(29).

Synthesis of 3: Et₂O (3 cm³) was added to Pu⁰ α -phase metal (0.0091 g, 0.038 mmol) followed by solid iodine addition (0.0195 g, 0.077 mmol) and the mixture stirred at ambient temperature for 36 h. The solvent was removed *in vacuo* to afford a red/brown residue. The residue was placed under thf (1.5 cm³) and two equiv (based on the assumption that 100% of the Pu⁰ starting material had reacted) of H^{Ar}acnac (0.0314 g, 0.076 mmol) and Na[N(SiMe₃)₂] (0.0140 g, 0.076 mmol) dissolved together in thf (1.5 cm³) were added. An immediate colour change was noted as a deep red solution formed. After stirring for 30

min, the solvent was removed *in vacuo* and the residue was dissolved in CH₂Cl₂ (1.5 cm³). The resulting intense deep red solution was filtered and stored at -35 °C overnight to yield dark crystals of PuI₂(^{Ar}acnac)₂ which were dried in vacuo (0.0089 g, 17% yield).

¹H NMR (CD₂Cl₂, 300 MHz): δ 8.45 (s, 4H, Ar CH), 7.63 (s, 4H, Ar CH), 7.48 (s, 4H, Ar CH), 6.95 (s, 4H, Ar CH), 6.46 (s, 4H, Ar CH), 6.37 (s, 2H, Ar CH), 6.33 (s, 4H, Ar CH), 3.68 (s, 2H, γ-CH), 0.86 (s, 36H, CMe₃). UV/vis/nIR: (in CH₂Cl₂) (nm); 255, 384. X-ray diffraction quality crystals for structural determination were obtained by recrystallisation from Et₂O at -35 °C.

Equipment and Instrumentation Details.

All uranium reactions and subsequent manipulations were performed under anaerobic and anhydrous conditions either under high vacuum or an atmosphere of nitrogen or argon. THF, hexanes, diethyl ether and toluene were dried using a Vacuum Atmospheres DRI-SOLV solvent purification system. C₆D₆ and CD₂Cl₂ were dried over activated 4Å and 3Å molecular sieves, respectively, for 24 h before use. UCl₄,^a UI₄(OEt₂)₂,^b and (^{Ar}acnac)H (Ar = 3,5-'Bu₂C₆H₃)^c were synthesized according to previously reported procedures. All other reagents were purchased from commercial suppliers and used as received. NMR spectra were recorded on a Varian UNITY INOVA 400 or Varian UNITY INOVA 500 spectrometer. ¹H NMR spectra were referenced to external SiMe₄ using the residual protio solvent peaks as internal standards. IR spectra were recorded on a Mattson Genesis FTIR spectrometer while UV-vis/NIR experiments were performed on a UV-3600 Shimadzu spectrophotometer. Elemental analyses were performed by the Microanalytical Laboratory at UC Berkeley. CV experiments were performed with a CH Instruments 600c Potentiostat, and the data were processed using CHI software (version 6.29). All experiments were performed in a glove box using a 20 mL glass vial as the cell. The working electrode consisted of a platinum disk embedded in glass (2 mm diameter), while platinum wire was used for both the counter and reference electrodes. Solutions employed during CV studies were typically 3 mM in the uranium complex and 0.1 M in [Bu₄N][PF₆]. All potentials are reported versus the [Cp₂Fe]^{0/+} couple. For all trials $i_{p,a}/i_{p,c} = 1$ for the [Cp₂Fe]^{0/+} couple, while $i_{p,c}$ increased linearly with the square root of the scan rate (i.e. \sqrt{v}). Redox couples which exhibited behavior similar to the [Cp₂Fe]^{0/+} couple were thus considered reversible. The solid-state molecular structure of complex **1** was determined as follows. Crystals were mounted on a glass fiber under Paratone-N oil. Data collection was carried out a Bruker 3-axis platform diffractometer with SMART-1000 CCD detector. The instrument was equipped with graphite monochromatized MoKα X-ray source ($\lambda = 0.71073 \text{ \AA}$). All data were collected at 150(2) K using Oxford nitrogen gas cryostream system. A hemisphere of data was collected using ω scans and 0.3° frame widths. A frame exposure of 10 seconds was used. SMART was used to determine the cell parameters and data collection. The raw frame data were processed using SAINT. The empirical absorption correction was applied based on Psi-scan. Subsequent calculations were carried out using SHELXTL. The structure was solved using Direct methods and difference Fourier techniques. All hydrogen atom positions were idealized, and rode on the atom of attachment. The final refinement included anisotropic temperature factors on all non-hydrogen atoms. Structure solution, refinement, graphics, and creation of publication materials for **1** were performed using SHELXTL. A crystal of **2** was mounted in a nylon cryoloop from Paratone-N oil under argon gas flow and shipped to Los Alamos National Laboratory for single crystal X-ray diffraction analysis. (**note that the X-ray diffraction data for**

the uranium compound **2** was obtained at LANL on the same diffractometer as **3** rather than at UCSB in order to allow the most accurate possible comparison of Pu(IV) vs U(IV) metrical parameters)

The plutonium chemistry was conducted at Los Alamos National Laboratory (LANL) inside a radiological facility approved and regulated to for the handling and manipulation of high specific-activity α -particle emitting radionuclides. α -phase Pu metal and acidic Pu stock solutions (used as a precursor to $[\text{PPh}_4]_2[\text{PuCl}_6]$) were obtained internally from LANL. All other chemicals were commercially obtained. Reactions with Pu and $^{4\alpha}\text{acnac}$ were performed inside a negative pressure helium atmosphere drybox (MBraun Labmaster 130). Solvents were purchased in anhydrous grade and stored over a 1:1 mixture of 3 and 4 Å dried molecular sieves inside the drybox before use. NMR spectra containing Pu were obtained on samples in 4 mm PTFE NMR tube liners inserted into 5mm NMR tubes to satisfy multiple containment safety requirements. NMR spectra of **3** were recorded on a Bruker Avance 300 MHz spectrometer. Electronic absorption spectra of **3** were recorded on a Varian Cary 6000i and Cary 500 UV/vis/nIR spectrophotometers.

Pu containing crystals of **3** were coated in Paratone-N oil and then mounted inside a 0.5 mm capillary tube. The capillaries were sealed with hot wax while inside the glovebox, and the external surface of the capillary coated with a thin film of acrylic in ethyl acetate (Hard as Nails[®] nail polish) outside the glovebox in order to provide appropriate containment of the transuranic isotope. The data were collected on a Bruker D8 diffractometer, with APEX II charge-coupled-device (CCD) detector, and Bruker Kryoflex low temperature device. The instrument was equipped with graphite monochromatized MoK α X-ray source ($\lambda = 0.71073 \text{ \AA}$), and a 0.5 mm monocapillary. A hemisphere of data was collected using ω scans, with 10-second frame exposures and 0.5° frame widths. Data collection and initial indexing and cell refinement were handled using APEX II^e software. Frame integration, including Lorentz-polarization corrections, and final cell parameter calculations were carried out using SAINT+^f software. The data were corrected for absorption using redundant reflections and the SADABS^g program. Decay of reflection intensity was not observed as monitored *via* analysis of redundant frames. The structure was solved using Direct methods and difference Fourier techniques. All hydrogen atom positions were idealized, and rode on the atom they were attached to. The final refinement included anisotropic temperature factors on all non-hydrogen atoms. For **2**, a disordered diethyl ether solvent molecule was treated using PLATON/SQUEEZE; the void was located at 0 0 0.5 (40 electrons, 193 \AA^{-3}). Structure solution, refinement, graphics, and creation of publication materials were performed using SHELXTL.^h

References from the above text:

- a J. L. Kiplinger, D. E. Morris, B. L. Scott and C. J. Burns, *Organometallics*, 2002, **21**, 5978.
- b D. D. Schnaars, G. Wu and T. W. Hayton, *Dalton Trans.*, 2008, 6121.
- c T. W. Hayton and G. Wu, *Inorg. Chem.*, 2009, **48**, 3065.
- d SMART Software Users Guide, 5.1; Bruker Analytical X-Ray Systems, Inc: Madison, WI, 1999.
- e SAINT Software Users Guide, 5.1; Bruker Analytical X-Ray Systems, Inc: Madison, WI, 1999.
- f Sheldrick, G. M. SHELXTL, 6.12; Bruker Analytical X-Ray Systems, Inc: Madison, WI, 2001.

e APEX II 1.08; Bruker AXS: Madison, WI, 2004.

f SAINT+ 7.06; Bruker AXS: Madison, WI, 2003.

g G. Sheldrick, SADABS 2.03; University of Göttingen, Göttingen, Germany, 2001.

h SHELXTL 5.10; Bruker AXS: Madison, WI, 1997.

Crystallographic Data for 1-3:

UCl₂(^{Ar}acnac)₂ (1): C₅₈H₆₄N₂O₂Cl₂U, $M = 1130.04$, triclinic, $a = 10.2220(16)$, $b = 11.5941(18)$, $c = 12.512(2)$ Å, $\alpha = 76.814(2)$, $\beta = 80.226(2)$, $\gamma = 65.223(2)$ °, $V = 1306.3(4)$ Å³, $T = 150(2)$ K, space group $P\overline{1}$, $Z = 1$, $\mu = 3.251$ mm⁻¹, reflections collected/independent = 10501/5108 [$R(\text{int}) = 0.0464$], $R_1(I > 2\sigma(I)) = 0.0458$, and $wR_2(I > 2\sigma(I)) = 0.0496$.

UI₂(^{Ar}acnac)₂·2CH₂Cl₂ (2): C₆₀H₆₈Cl₄I₂N₂O₂U, $M = 1482.79$, monoclinic, $a = 11.5036(13)$, $b = 20.834(2)$, $c = 12.6003(14)$ Å, $\alpha = 90$, $\beta = 95.737(1)$, $\gamma = 90$ °, $V = 3004.7(6)$ Å³, $T = 140(1)$ K, space group $P2_1/c$, $Z = 2$, $\mu = 3.948$ mm⁻¹, reflections collected/independent = 28627/5531 [$R(\text{int}) = 0.0623$], $R_1(I > 2\sigma(I)) = 0.0380$, and $wR_2(I > 2\sigma(I)) = 0.0863$.

PuI₂(^{Ar}acnac)₂·Et₂O (3): C₆₂H₇₄N₂O₃I₂Pu, $M = 1388.09$, triclinic, $a = 10.1318(10)$, $b = 11.8288(11)$, $c = 13.1117(13)$ Å, $\alpha = 105.2990(10)$, $\beta = 103.8160(10)$, $\gamma = 93.7570(10)$ °, $V = 1457.9(2)$ Å³, $T = 140(1)$ K, space group $P\overline{1}$, $Z = 1$, $\mu = 2.233$ mm⁻¹, reflections collected/independent = 16551/6681 [$R(\text{int}) = 0.0236$], $R_1(I > 2\sigma(I)) = 0.0238$, and $wR_2(I > 2\sigma(I)) = 0.0560$.

Photographs of Experimental Set-Up:

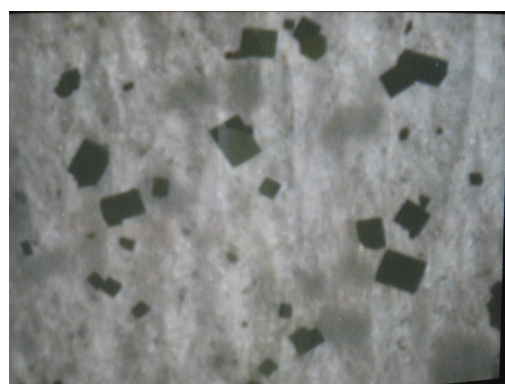


Figure S1. Photograph of single crystals of PuI₂(^{Ar}acnac)₂ (compound 3) taken from a monitor image of the crystals under a microscope fitted to a closed circuit camera device inside a negative pressure helium atmosphere drybox.



Figure S2. Photograph showing the set-up used to mount the crystals of **3** into a capillary tube. A microscope is needed inside the dry-box as part of the contamination control and safety procedures required when handling the ^{239}Pu radioisotope.

Solid State Molecular Structures

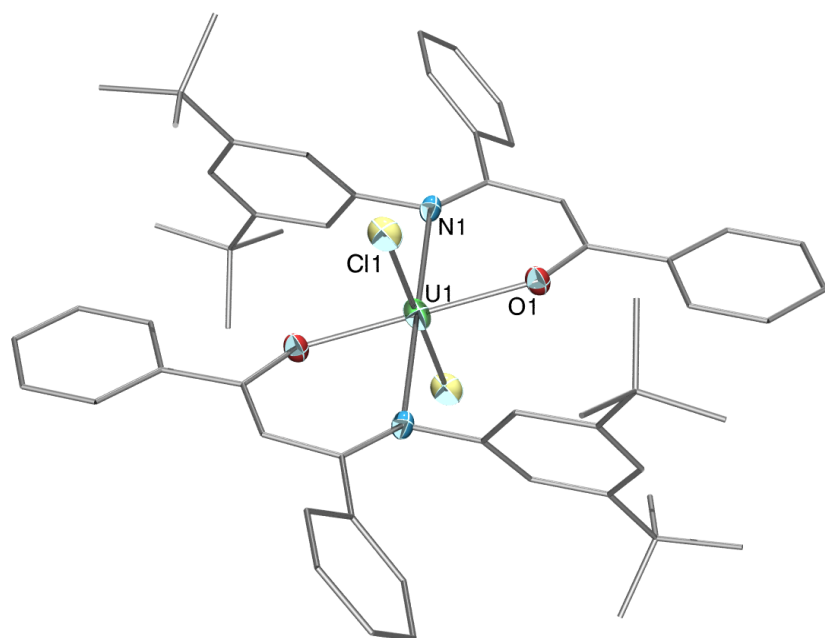


Figure S3. Solid-state structure of $\text{UCl}_2(^{\text{Ar}}\text{acnac})_2$ (**1**) with 50% probability ellipsoids.

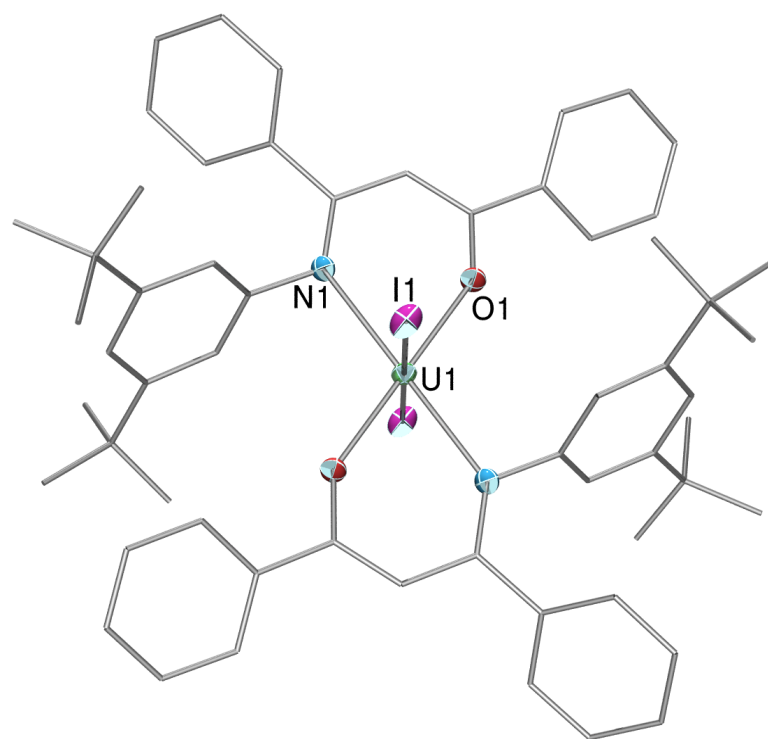


Figure S4. Solid-state structure of $\text{UI}_2(\text{Aracnac})_2 \cdot 2\text{CH}_2\text{Cl}_2$ (**2**) with 50% probability ellipsoids.

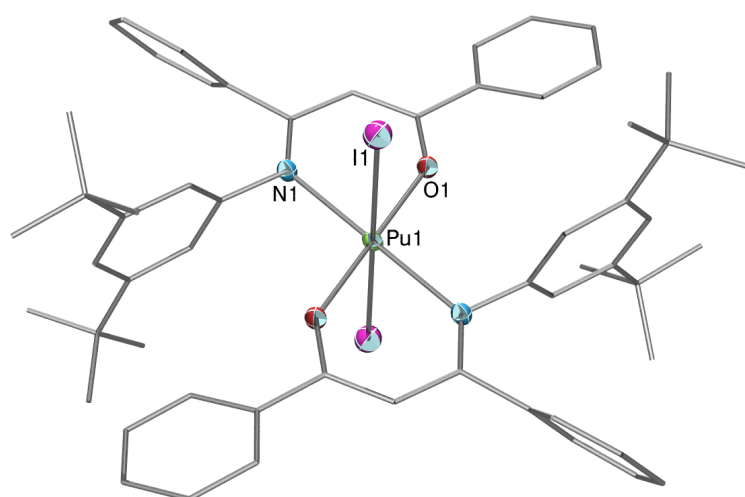


Figure S5. Solid-state structure of $\text{PuI}_2(\text{Aracnac})_2 \cdot \text{Et}_2\text{O}$ (**3**) with 50% probability ellipsoids.

NMR Data

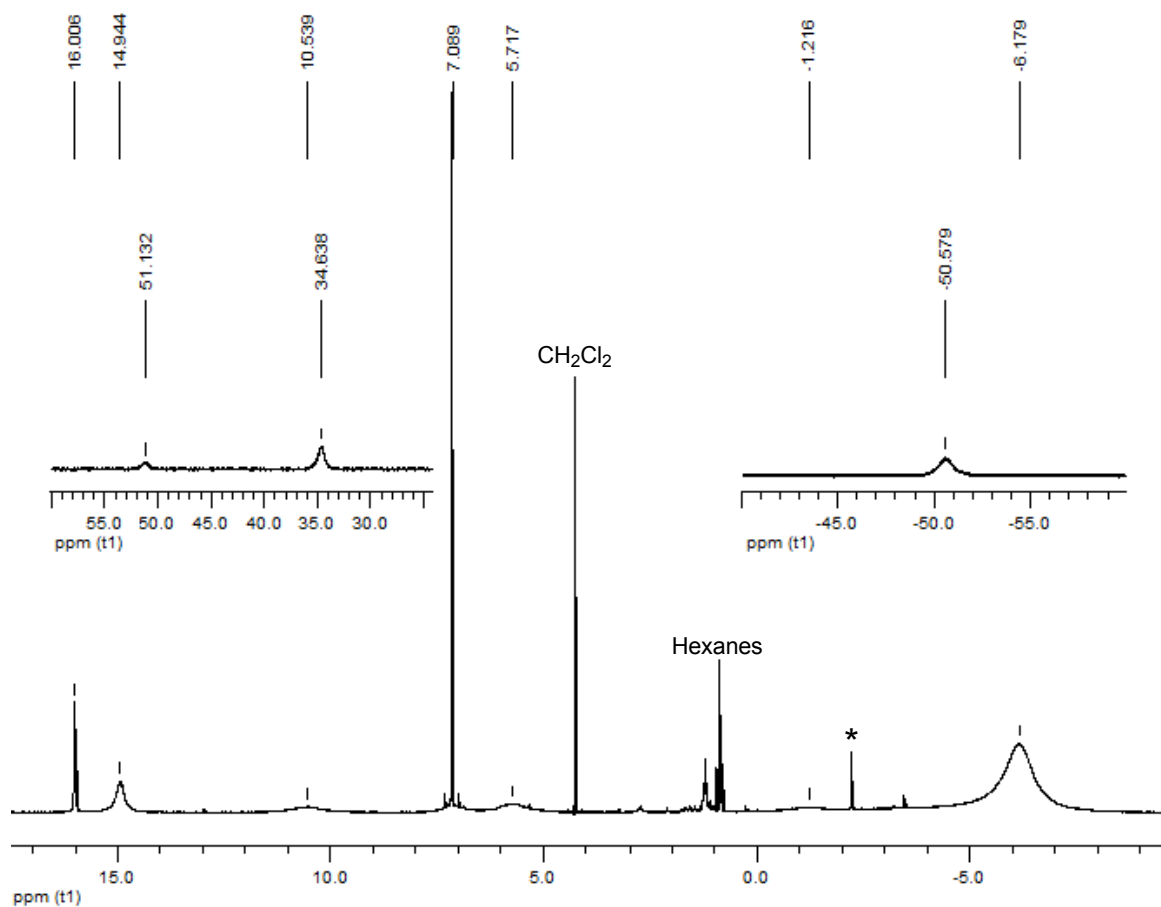


Figure S6A. ¹H NMR spectrum of **1** in C_6D_6 . * denotes a minor impurity.

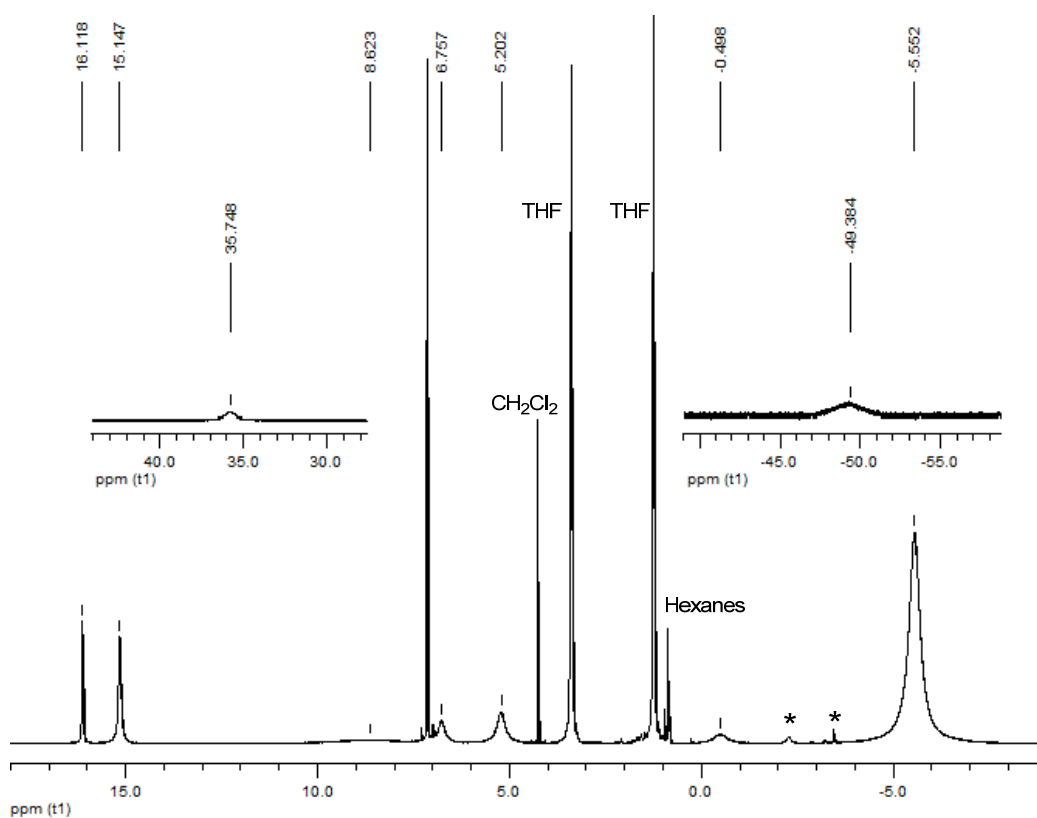


Figure S6B. ¹H NMR spectrum of **1** in C_6D_6 (the above sample from Fig 6A) with 1 equiv THF added. The ortho CH resonance previously found at 10.54 ppm and the N-aryl ortho CH resonance previously found at -50.58 ppm have broadened and are now located at 8.62 ppm and -49.38 ppm respectively. The N-aryl para CH resonance previously found at 51.13 ppm has also broadened and is no longer observed. * denotes a minor impurity.

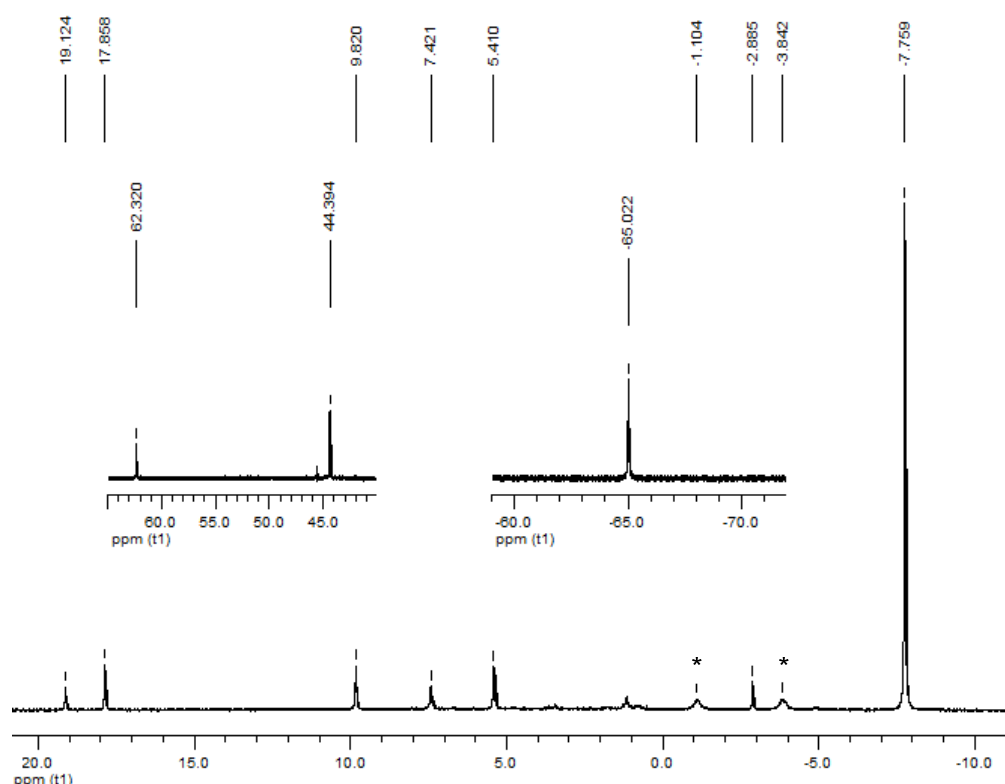


Figure S7. ¹H NMR spectrum of **2** in CD₂Cl₂. * indicates the resonances assigned to the minor *cis* isomer

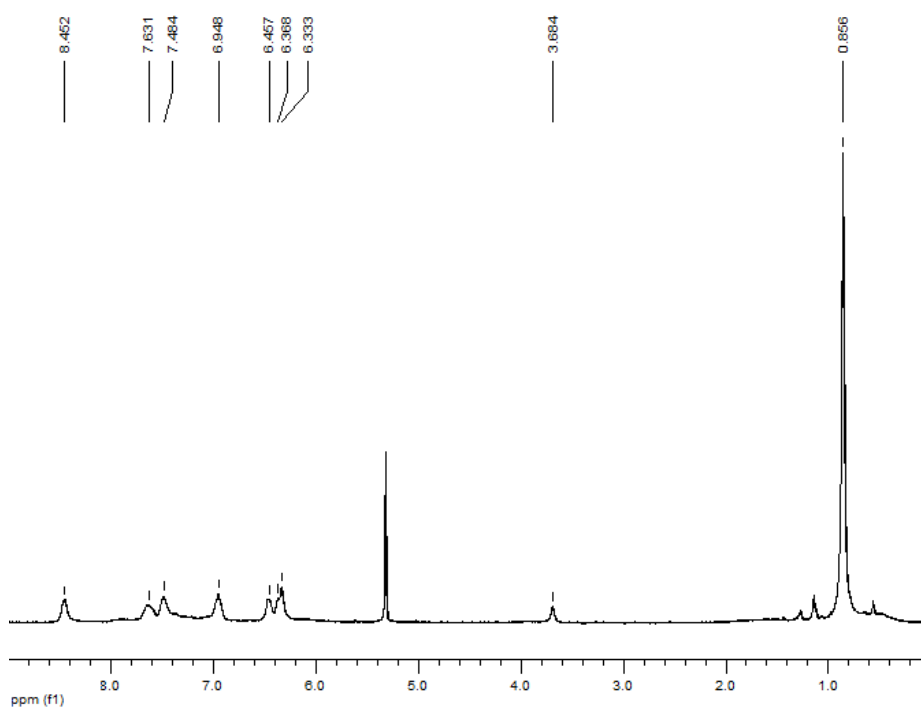


Figure S8. ¹H NMR spectrum of **3** in CD₂Cl₂.

UV/vis/nIR data

Electronic absorption spectra of **1** and **2** in CH_2Cl_2 solution contain observable f-f/f-d transitions along with strong charge transfer bands dominating out to beyond 700 nm. Although U(IV)-halide charge transfer bands have been known for a long time and are well documented in complexes such as $[\text{UCl}_6]^{2-}$, they do not account for the intensity of those observed in **1** and **2**, which we believe arise from the ${}^{\text{Ar}}\text{acnac}$ ligand. For the Pu(IV) complex **3** the solution UV/vis/nIR spectrum in CH_2Cl_2 is dominated by intense charge transfer transitions, with no observable f-f/f-d transitions (masked by the strong intensity of charge transfer bands involving the ${}^{\text{Ar}}\text{acnac}$ and iodide ligands).ⁱ

ⁱ J. L. Ryan and C. K. Jørgensen, *Mol. Phys.*, 1964, **7**, 17.



Figure S9. UV-Vis/NIR spectrum of **1** (CH_2Cl_2 , 4.32×10^{-3} M). Solvent absorption has been removed for clarity.

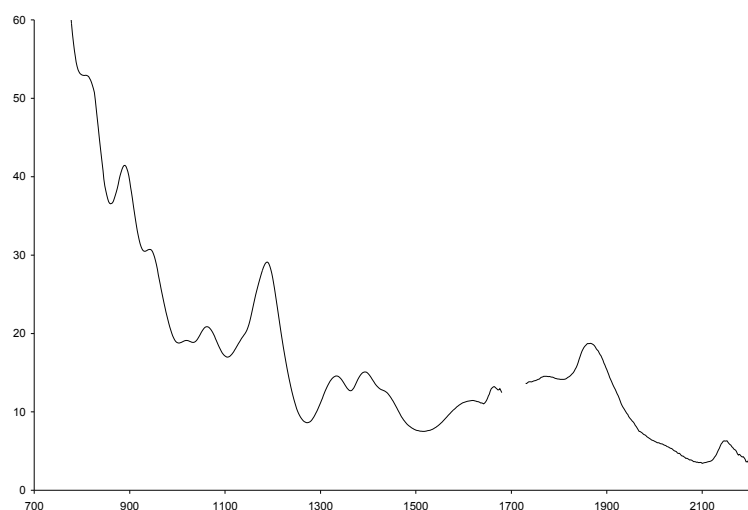


Figure S10. UV-Vis/NIR spectrum of **2** (CH_2Cl_2 , 4.39×10^{-3} M). Solvent absorption has been removed for clarity.

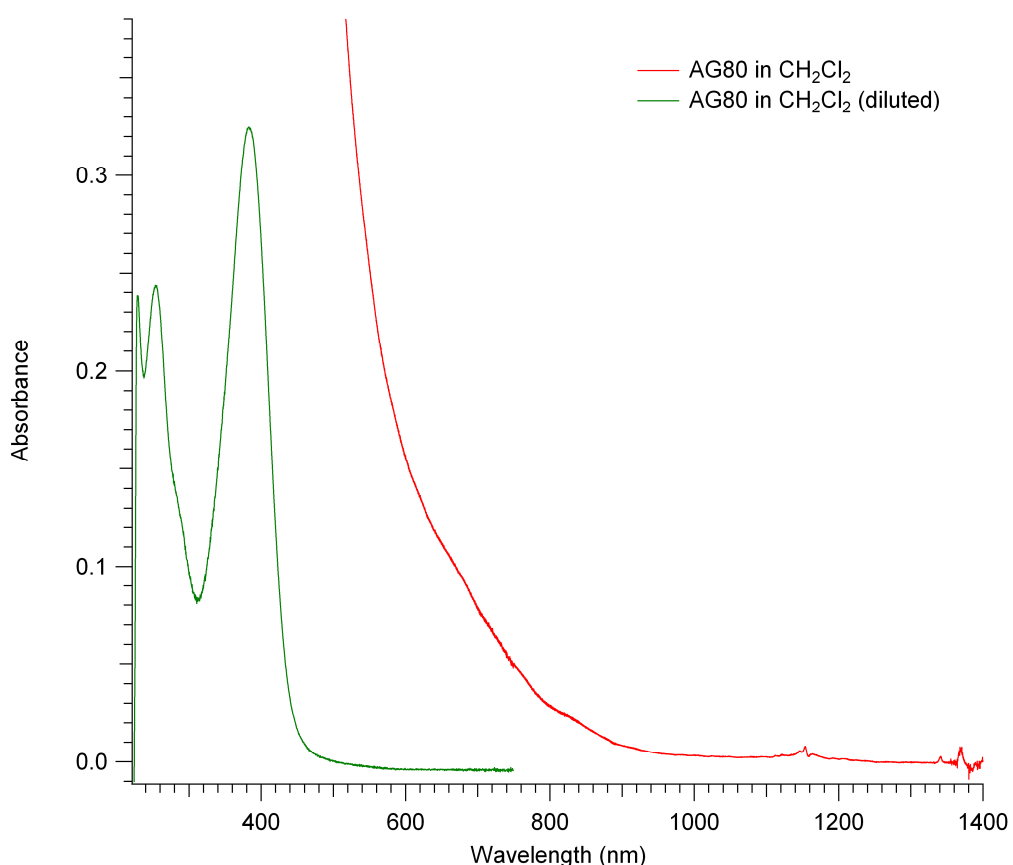


Figure S11: UV-vis/nIR spectra of $\text{PuI}_2(\text{Aracnac})_2$ (**3**). The red line shows **3** dissolved in CH_2Cl_2 and the green line shows **3** dissolved in CH_2Cl_2 at a more dilute concentration to allow resolution of the charge transfer maxima.

IR data

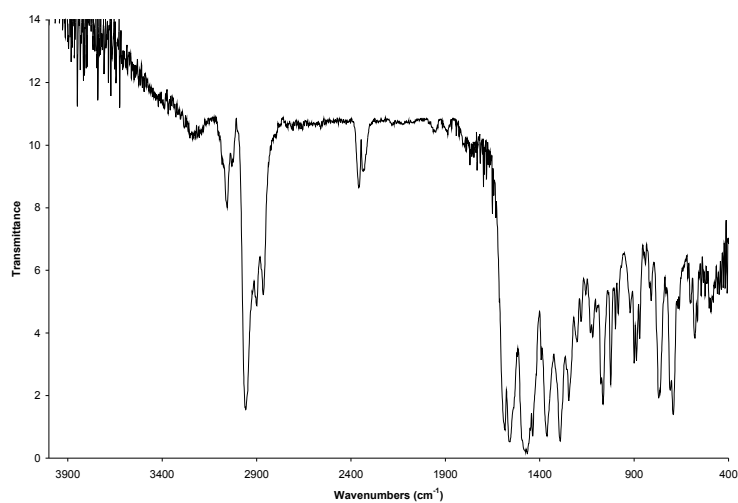


Figure S12. IR spectrum of complex **1** (as KBr mull).

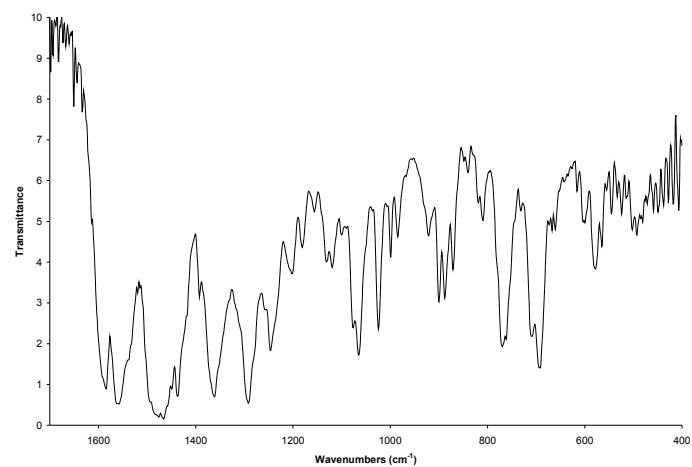


Figure S13. Expanded IR spectrum of complex **1** (as KBr mull).

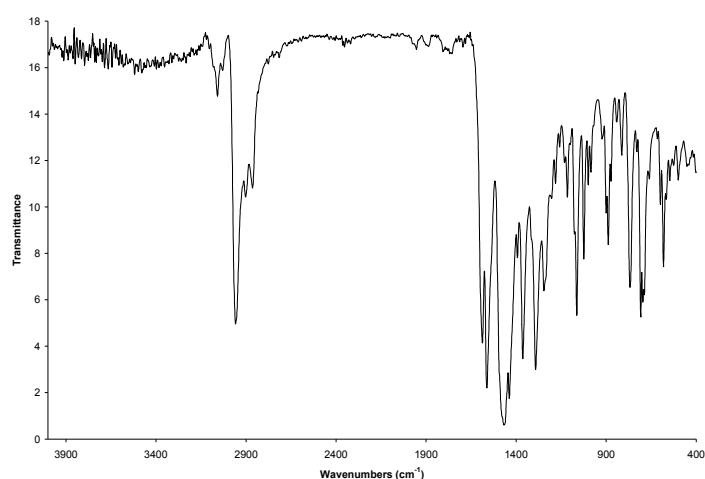


Figure S14. IR spectrum of complex **2** (as KBr mull).

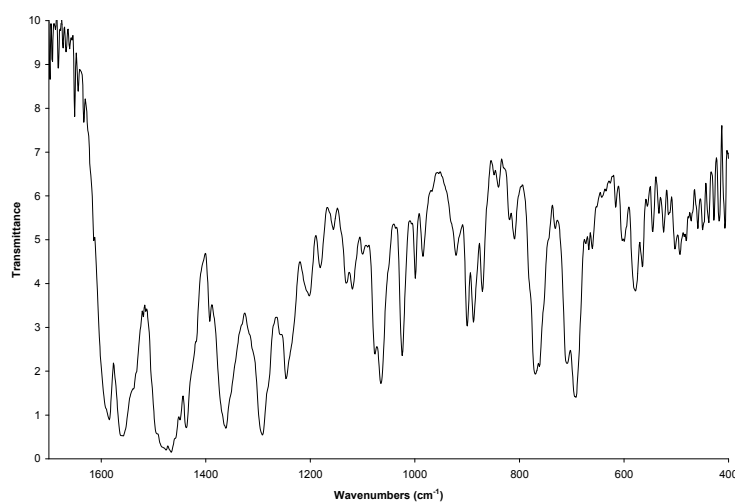


Figure S15. Expanded IR spectrum of complex **2** (as KBr mull).

Electrochemistry

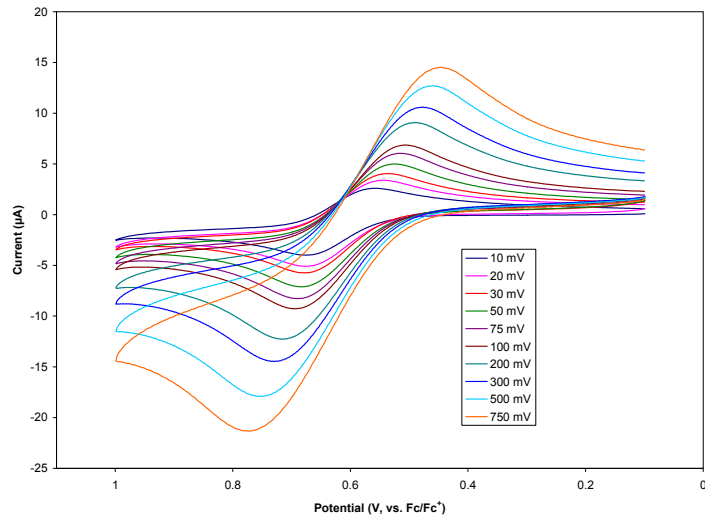


Figure S16. Room temperature cyclic voltammogram for **1** in CH_2Cl_2 (0.1 M $[\text{NBu}_4]\text{[PF}_6]$ as supporting electrolyte). The U(IV)/U(V) redox couple is at $E_{1/2} = 0.601$ V with a scan rate of 100 mV/s.

Table S1. Electrochemical parameters for complex **1** in CH_2Cl_2 (vs. Fc/Fc^+ , $[\text{NBu}_4]\text{[PF}_6]$ as supporting electrolyte).

Oxidation Feature	Scan rate, V/s	$E_{p,c}$, V	$E_{p,a}$, V	ΔE_p^a	$i_{p,c}/i_{p,a}$
	0.01	0.558	0.675	0.117	0.86
	0.02	0.544	0.675	0.131	0.90
	0.03	0.536	0.679	0.143	0.92
	0.05	0.524	0.683	0.159	0.91
	0.075	0.514	0.688	0.174	0.91
	0.10	0.507	0.695	0.188	0.91
	0.20	0.489	0.717	0.228	0.88
	0.30	0.476	0.729	0.253	0.85
	0.50	0.459	0.751	0.292	0.80
	0.75	0.446	0.771	0.325	0.74

^a ΔE_p is defined as the potential difference between the cathodic wave and the anodic wave generate after the change in sweep direction.

Computational Methodology and Results in More Detail

All the theoretical calculations were performed using hybrid density functional theory with the B3LYP functional^j as implemented in Gaussian 09 rev. B.01.^k For hydrogen and carbon we used the 6-31g* basis set while for the oxygen and nitrogen atoms, that are directly coordinated to the An the larger basis set 6-311++g(3df) was used. The iodine atoms were described with the lanl2 relativistic effective core potential^l (RECP) and its associated basis set, and for the U and Pu we used the small core SDD RECP^m that puts 60 electrons in the core (shells 1 through 4). The geometry optimizations were carried out with no constraints and for the natural bond orbital analysis we used NBO 5.0 as implemented in link 607 for Gaussian 09.

Computational References from the above text:

[j] C. Lee, W. Yang, and R. G. Parr, *Phys. Rev. B*, 1988, **37**, 785; A. D. Becke, *J. Chem. Phys.*, 1993, **98**, 5648.

[k] Gaussian 09, Revision B.01, M. J. Frisch, G. W. Trucks, H. B. Schlegel, G. E. Scuseria, M. A. Robb, J. R. Cheeseman, G. Scalmani, V. Barone, B. Mennucci, G. A. Petersson, H. Nakatsuji, M. Caricato, X. Li, H. P. Hratchian, A. F. Izmaylov, J. Bloino, G. Zheng, J. L. Sonnenberg, M. Hada, M. Ehara, K. Toyota, R. Fukuda, J. Hasegawa, M. Ishida, T. Nakajima, Y. Honda, O. Kitao, H. Nakai, T. Vreven, J. A. Montgomery, Jr., J. E. Peralta, F. Ogliaro, M. Bearpark, J. J. Heyd, E. Brothers, K. N. Kudin, V. N. Staroverov, T. Keith, R. Kobayashi, J. Normand, K. Raghavachari, A. Rendell, J. C. Burant, S. S. Iyengar, J. Tomasi, M. Cossi, N. Rega, J. M. Millam, M. Klene, J. E. Knox, J. B. Cross, V. Bakken, C. Adamo, J. Jaramillo, R. Gomperts, R. E. Stratmann, O. Yazyev, A. J. Austin, R. Cammi, C. Pomelli, J. W. Ochterski, R. L. Martin, K. Morokuma, V. G. Zakrzewski, G. A. Voth, P. Salvador, J. J. Dannenberg, S. Dapprich, A. D. Daniels, O. Farkas, J. B. Foresman, J. V. Ortiz, J. Cioslowski, and D. J. Fox, Gaussian, Inc., Wallingford CT, 2010.

[l] P.J. Hay and W.R. Wadt, *J. Chem. Phys.*, 1985, **82**, 299

[m] X. Cao, M. Dolg, and H. Stoll, *J. Chem. Phys.*, 2003, **118**, 487; W. Küchle, M. Dolg, H. Stoll, and H. Preuss, *J. Chem. Phys.*, 1994, **100**, 7535

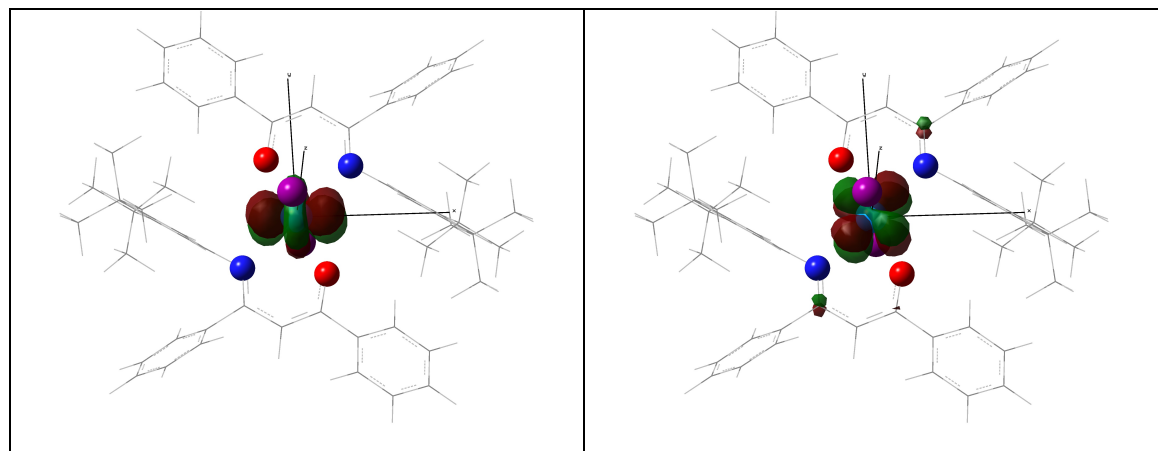


Figure S17. Unpaired spin density in $\text{UI}_2(\text{Ar}-\text{acnac})_2$ (**2**).

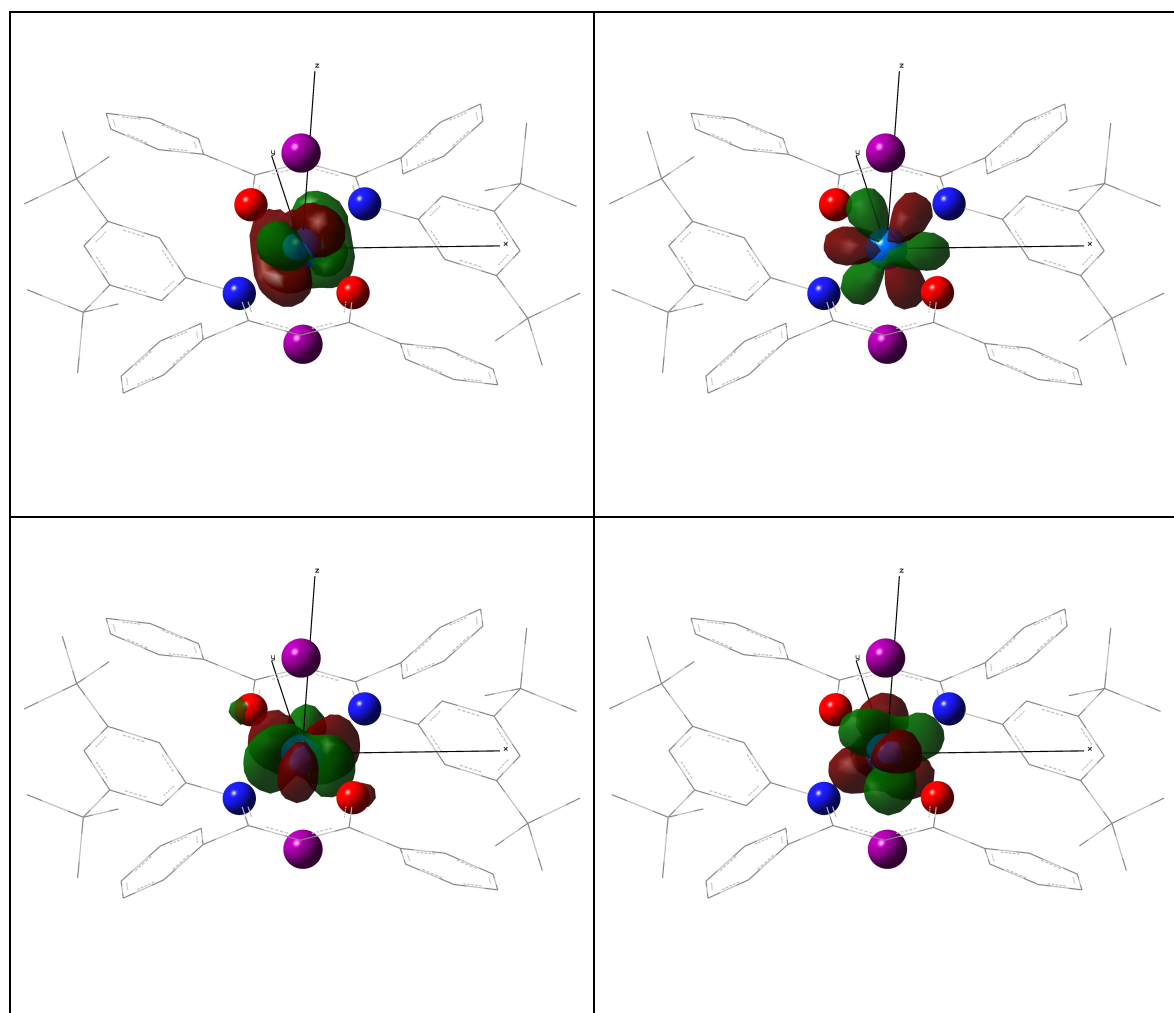


Figure S18. Unpaired spin density in $\text{PuI}_2(\text{Ar}-\text{acnac})_2$ (**3**).

Selected Natural Atomic Orbitals with strongest interaction in 2nd order perturbation theory treatment:

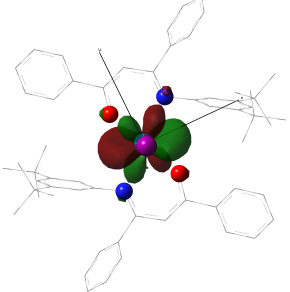
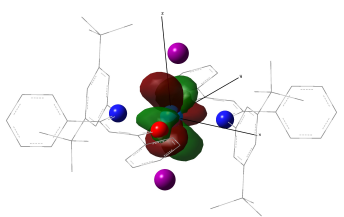
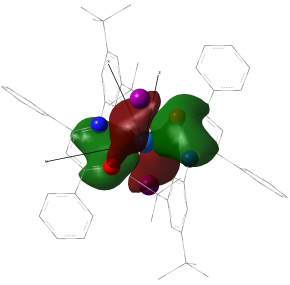
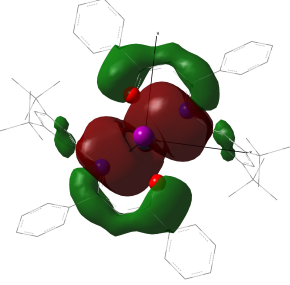
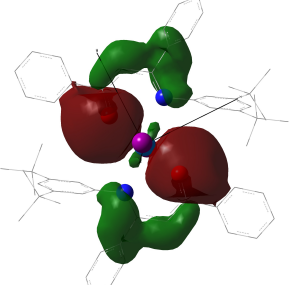
UL₂(^{Ar}acnac)₂(2):

O:LP ₁	40% s + 60% p	
O:LP ₂	16% s + 84% p	
O:LP ₃	100% p	

Figure S19. Oxygen lone pairs.

N:LP ₁	25% s + 75% p	
-------------------	---------------	--

Figure S20. Nitrogen lone pair.

U:LP* ₄	100% f	
U:LP* ₅	100% f	
U:LP* ₆	100% d	
U:LP* ₈	34% s + 66% d	
U:LP* ₁₀	30% s + 70% d	

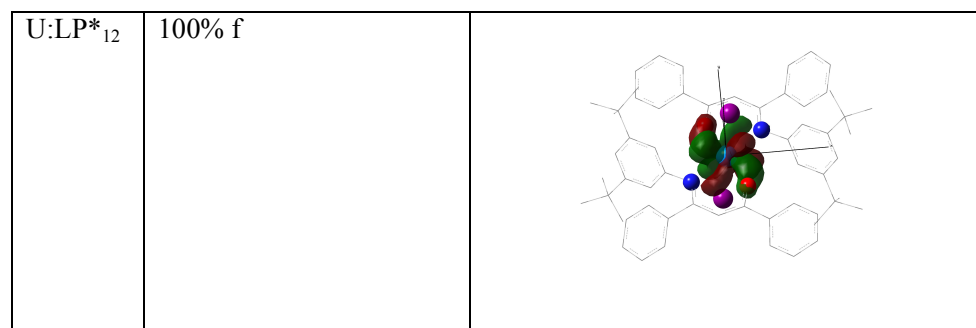


Figure S21. Uranium virtual lone pairs.

$$\text{Interaction energies: } \Delta E^{(2)} = \frac{\left| \langle \varphi_d | F | \varphi_a \rangle \right|^2}{\varepsilon_a - \varepsilon_d}$$

		$\Delta E^{(2)}$
U-N	N:LP ₁ → U:LP* ₄	8 kcal/mol
	N:LP ₁ → U:LP* ₈	25 kcal/mol
U-O	O:LP ₁ → U:LP* ₁₀	23 kcal/mol
	O:LP ₂ → U:LP* ₄	13 kcal/mol
	O:LP ₂ → U:LP* ₁₀	15 kcal/mol
	O:LP ₃ → U:LP* ₆	5.5 kcal/mol
	O:LP ₃ → U:LP* ₅	4.7 kcal/mol
	O:LP ₁ → U:LP* ₁₂	4.3 kcal/mol

Table S2. Metal-ligand interaction energies in $\text{UI}_2(\text{^Aracnac})_2$ (**2**)

PuI₂(^{Ar}acnac)₂ (3):

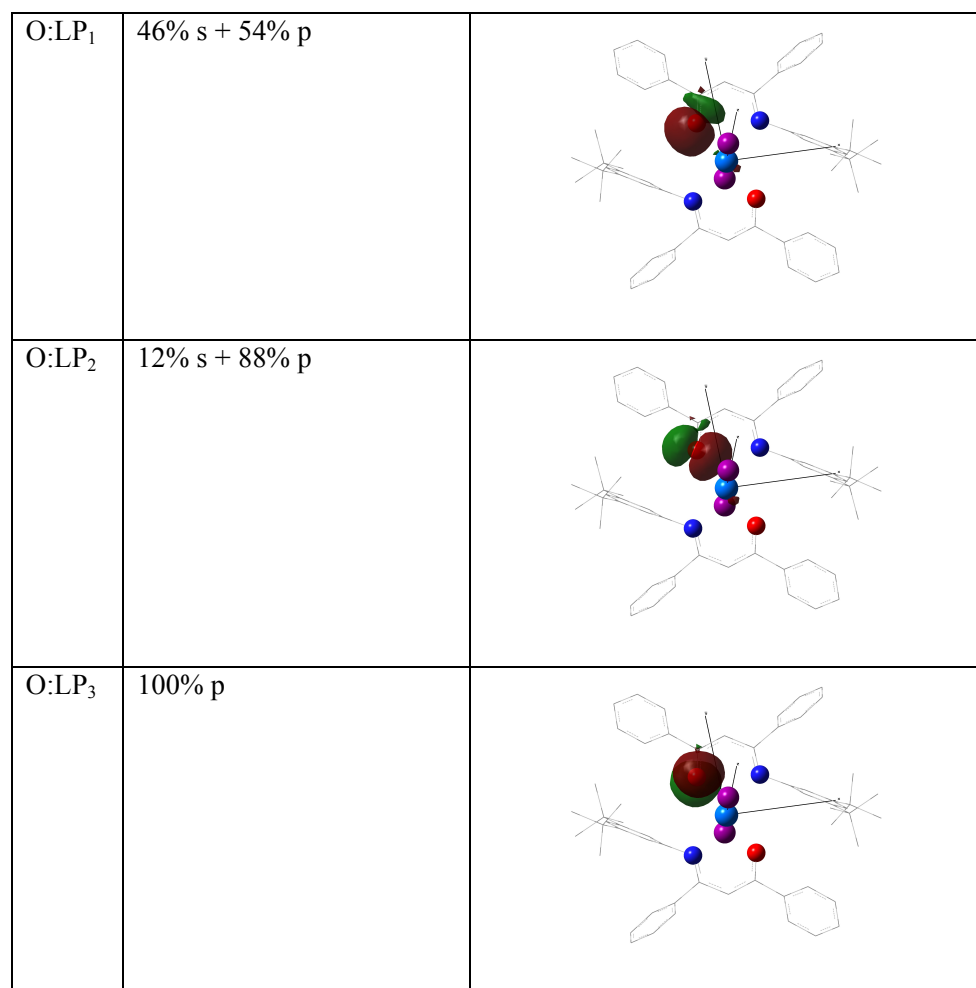


Figure S22. Oxygen lone pairs.

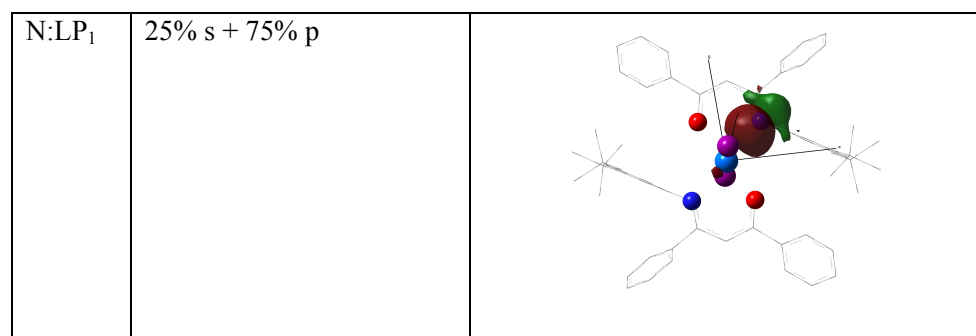


Figure S23. Nitrogen lone pair.

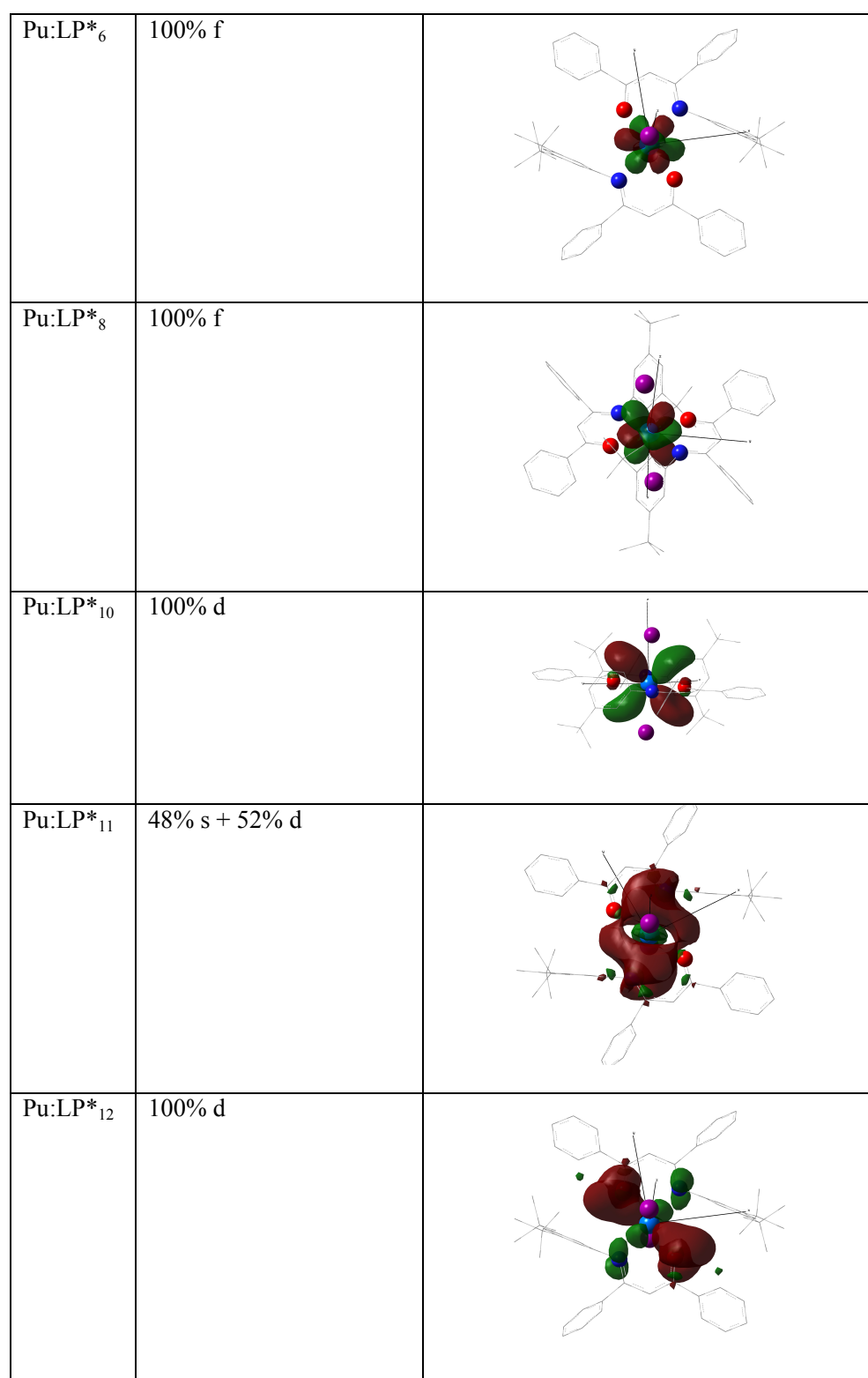


Figure S24. Plutonium virtual lone pairs.

Interaction energies: $\Delta E^{(2)} = \frac{|\langle \varphi_d | F | \varphi_a \rangle|^2}{\epsilon_a - \epsilon_d}$

		$\Delta E^{(2)}$
Pu-N	N:LP ₁ → Pu:LP* ₆	7 kcal/mol
	N:LP ₁ → Pu:LP* ₁₁	21 kcal/mol
Pu-O	O:LP ₁ → Pu:LP* ₁₂	16.5 kcal/mol
	O:LP ₂ → Pu:LP* ₁₂	8.9 kcal/mol
	O:LP ₂ → Pu:LP* ₆	6.5 kcal/mol
	O:LP ₂ → Pu:LP* ₁₁	5.7 kcal/mol
	O:LP ₂ → Pu:LP* ₈	5.4 kcal/mol
	O:LP ₃ → Pu:LP* ₁₀	6.1 kcal/mol

Table S3. Metal-ligand interaction energies in $\text{PuI}_2(^{\text{Ar}}\text{acnac})_2$ (**3**)

Coordinates used for optimized geometries:

Cartesian coordinates of the DFT-optimized $\text{UI}_2(^{\text{Ar}}\text{acnac})_2$ (**2**)

U	0.00029100	0.00259000	-0.00021100
I	0.32033700	0.52566400	-3.01105100
O	0.89344200	-1.97830300	-0.23264400
C	-3.46265600	-0.03366100	-1.38252600
H	-2.84903000	-0.01187500	-2.27736800
N	-1.83458500	-1.58540300	-0.41901700
C	-1.84781000	-2.90299900	-0.49963200
C	-4.65131400	0.71445100	-1.29960300
C	-5.00630500	-0.17737000	0.97224800
C	-5.39784400	0.62134300	-0.12044600

H -6.32178100 1.18143700 -0.04054900
C -4.03102900 -3.48256500 -1.65320000
H -3.81450700 -2.74098000 -2.41480300
C -3.13114400 -3.67706100 -0.59523900
C -5.09962300 1.56321000 -2.50561300
C -5.28042200 -1.14284300 3.32670900
H -5.16808900 -2.18019200 2.99138400
H -5.93834200 -1.15041300 4.20322000
H -4.29854400 -0.77964100 3.64971500
C -3.82072000 -0.90309100 0.85863200
H -3.46586900 -1.52835000 1.66715200
C -3.06266300 -0.84801200 -0.32206800
C 1.70027500 -5.52938700 -0.27109200
H 0.76309900 -5.95042400 0.07839800
C -5.89386200 -0.25077700 2.22984100
C 3.03948200 -3.62483200 -0.93250000
H 3.12625100 -2.56173400 -1.12549700
C 1.79936500 -4.15133000 -0.53352700
C -0.66691500 -3.70426700 -0.52507300
H -0.81827300 -4.75737200 -0.71629400
C 0.63104800 -3.24346300 -0.41635200
C 4.14307000 -4.46154000 -1.09210700
H 5.09023500 -4.04171300 -1.41848200
C -6.40520900 2.33262800 -2.22784900
H -6.29828900 3.02186300 -1.38227700
H -7.24411000 1.65825900 -2.01951100

H -6.67329800 2.92862500 -3.10732100
C -5.19571600 -4.24563300 -1.73379100
H -5.88077400 -4.09251500 -2.56309100
C -3.41333500 -4.65429700 0.37120600
H -2.71527100 -4.81399800 1.18851500
C -5.48171900 -5.20112300 -0.75592400
H -6.39362200 -5.78870900 -0.81817100
C -6.08969600 1.16635100 2.81890900
H -5.12980300 1.60506800 3.11491300
H -6.72942500 1.12274100 3.70876400
H -6.56697800 1.84372000 2.10229200
C -4.58859600 -5.40262500 0.29814300
H -4.80287800 -6.14507400 1.06208400
C -7.27169300 -0.83919700 1.84192300
H -7.78535600 -0.22069600 1.09794100
H -7.91929900 -0.90679800 2.72491200
H -7.16194000 -1.84576000 1.42228000
C 2.80805000 -6.35982300 -0.41993700
H 2.71764200 -7.42076300 -0.20394800
C -4.00092200 2.59319200 -2.86115300
H -3.81608100 3.27309400 -2.02264500
H -4.31374600 3.19380900 -3.72443400
H -3.05190000 2.11275400 -3.11828200
C -5.33864800 0.63206600 -3.71853100
H -5.66072200 1.21662300 -4.58898800
H -6.11790600 -0.10765400 -3.49950000

H -4.42888600 0.09204600 -4.00103200
C 4.03180000 -5.83030600 -0.83835100
H 4.89396100 -6.48051400 -0.95960800
I -0.31973100 -0.52001800 3.01088700
O -0.89121400 1.98443700 0.23165300
C 3.46010600 0.03377900 1.38466100
H 2.84621700 0.01515600 2.27940700
N 1.83657200 1.58820800 0.41878700
C 1.85152200 2.90585300 0.49863100
C 4.64545300 -0.71958300 1.30247200
C 5.00278300 0.16640400 -0.97124200
C 5.39136700 -0.63233700 0.12250200
H 6.31232300 -1.19731800 0.04264200
C 4.03384100 3.48389300 1.65464200
H 3.81552600 2.74301400 2.41639900
C 3.13562200 3.67855500 0.59526600
C 5.08949900 -1.56961500 2.50915200
C 5.27849900 1.12424900 -3.32860200
H 5.17255700 2.16308800 -2.99582300
H 5.93501000 1.12578600 -4.20620000
H 4.29406400 0.76573000 -3.64906700
C 3.82080900 0.89807000 -0.85802600
H 3.46779600 1.52275500 -1.66780800
C 3.06311200 0.84819300 0.32314100
C -1.69193100 5.53707800 0.26671900
H -0.75402500 5.95579700 -0.08358300

C 5.88869100 0.23159500 -2.23040300
C -3.03479600 3.63601400 0.93069600
H -3.12369300 2.57332700 1.12495900
C -1.79374600 4.15948200 0.53068100
C 0.67157800 3.70853300 0.52279700
H 0.82423000 4.76155900 0.71338100
C -0.62704900 3.24940000 0.41449400
C -4.13652900 4.47526600 1.08989200
H -5.08439600 4.05784700 1.41724500
C 6.38264300 -2.35813300 2.22673900
H 6.25988200 -3.05239900 1.38746600
H 7.22846500 -1.69633300 2.00635400
H 6.65014600 -2.95092100 3.10855400
C 5.19907600 4.24598500 1.73647800
H 5.88277800 4.09277700 2.56687800
C 3.42002900 4.65509500 -0.37124600
H 2.72324900 4.81499700 -1.18960900
C 5.48733000 5.20065800 0.75847600
H 6.39965300 5.78748700 0.82169500
C 6.07522200 -1.18826900 -2.81595300
H 5.11234400 -1.62174800 -3.10999900
H 6.71445000 -1.15099400 -3.70645500
H 6.54882000 -1.86676600 -2.09793100
C 4.59587500 5.40238300 -0.29695400
H 4.81189500 6.14423600 -1.06098600
C 7.27055800 0.81307100 -1.84637200

H	7.78191200	0.19364000	-1.10157900
H	7.91704600	0.87452300	-2.73062700
H	7.16733100	1.82138700	-1.42929700
C	-2.79788400	6.37000500	0.41506500
H	-2.70533400	7.43051700	0.19788300
C	3.97865300	-2.58271500	2.87521200
H	3.78003400	-3.26384700	2.04086600
H	4.28761300	-3.18358100	3.73971700
H	3.03774800	-2.08782400	3.13488600
C	5.34859900	-0.63725500	3.71701200
H	5.66894500	-1.22281500	4.58742600
H	6.13588300	0.09150400	3.49007900
H	4.44785400	-0.08452100	4.00370300
C	-4.02254100	5.84350700	0.83458900
H	-4.88326800	6.49565200	0.95561200

Cartesian coordinates of the DFT-optimized PuI₂(^{Ar}acnac)₂ (**3**)

Pu	0.00019100	0.00039500	-0.00343900
I	0.30110800	0.53998800	-2.98513800
O	-1.00863300	1.93890100	0.23608600
N	1.79860000	1.56876900	0.41215900
C	3.04897600	0.86908400	0.32402200
C	3.46534100	0.07337500	1.39196000
H	2.84635800	0.03868500	2.28270000

C 4.67022700 -0.64835300 1.31947200
C 5.41848900 -0.54820700 0.14199900
H 6.35351700 -1.09076400 0.06787500
C 5.01280900 0.23370100 -0.95718400
C 3.81133100 0.93480700 -0.85285400
H 3.44339500 1.54200500 -1.66937400
C 5.12929800 -1.48206500 2.53149100
C 5.35121600 -0.54086400 3.73993000
H 6.11966300 0.20951300 3.51877700
H 5.67972900 -1.11601500 4.61416300
H 4.43277100 -0.01285100 4.01709600
C 4.04508700 -2.52652600 2.89066800
H 3.08936700 -2.05820100 3.14582800
H 4.36644900 -3.11999200 3.75574800
H 3.86943800 -3.21082000 2.05379900
C 6.44709600 -2.23340600 2.26133000
H 6.35227300 -2.93070200 1.42082900
H 6.72332500 -2.81886800 3.14541900
H 7.27575800 -1.54770400 2.04900800
C 5.89919000 0.30665600 -2.21499100
C 6.08337700 -1.11278200 -2.80334800
H 6.54969900 -1.79454700 -2.08324600
H 6.72751200 -1.07631300 -3.69037200
H 5.12028100 -1.54205600 -3.10293100
C 7.28283300 0.88705600 -1.83008700
H 7.17893100 1.88437700 -1.38735200

H 7.92045900 0.97540200 -2.71823800
H 7.80575000 0.25379900 -1.10556900
C 5.28860900 1.20243200 -3.31062000
H 4.30813700 0.84025900 -3.63923800
H 5.94958300 1.21315600 -4.18485700
H 5.17489700 2.23826300 -2.97118200
C 1.76758500 2.88885200 0.48503300
C 3.03056500 3.69748900 0.58154900
C 3.92576400 3.53670300 1.64866700
H 3.72379900 2.79458900 2.41387900
C 5.06753300 4.33323400 1.73311600
H 5.74938200 4.20613700 2.56942500
C 5.33467100 5.28913000 0.75029400
H 6.22891400 5.90294800 0.81560600
C 4.44584100 5.45650100 -0.31328400
H 4.64557100 6.19894500 -1.08117100
C 3.29319400 4.67404300 -0.39071300
H 2.59732600 4.80743400 -1.21457800
C 0.57285400 3.66367900 0.50896000
H 0.71062200 4.71974200 0.69406800
C -0.72869600 3.19245500 0.41237000
C -1.89071400 4.11316800 0.53599600
C -1.79045600 5.48682300 0.25457600
H -0.85612400 5.90098300 -0.11046100
C -2.89490200 6.32216900 0.40442300
H -2.80435200 7.37998300 0.17352300

C -4.11520900 5.80133300 0.84276000
H -4.97440900 6.45543200 0.96446200
C -4.22760500 4.43607300 1.11535000
H -5.17287900 4.02293500 1.45593000
C -3.12770200 3.59509200 0.95474900
H -3.21299800 2.53401500 1.15893000
I -0.30049100 -0.53932800 2.97821800
O 1.00903100 -1.93786900 -0.24571300
N -1.79871100 -1.56768400 -0.41743200
C -3.04921000 -0.86928900 -0.32081200
C -3.46903300 -0.06498000 -1.38093500
H -2.85241200 -0.02212200 -2.27293400
C -4.67404900 0.65555800 -1.29881300
C -5.41939800 0.54442800 -0.12050000
H -6.35449900 1.08585700 -0.03924300
C -5.01008500 -0.24617300 0.97104300
C -3.80806300 -0.94492500 0.85774600
H -3.43736200 -1.55855500 1.66819600
C -5.13630500 1.50079400 -2.50151600
C -5.34057200 0.57433700 -3.72436400
H -6.10172200 -0.18767000 -3.51828300
H -5.67055000 1.15802900 -4.59236100
H -4.41459100 0.06066700 -4.00344000
C -4.06255300 2.56300900 -2.83951400
H -3.09999100 2.10982900 -3.09623600
H -4.38631900 3.16532100 -3.69755100

H -3.89942200 3.23700000 -1.99175800
C -6.46428200 2.23272700 -2.22798000
H -6.38300100 2.91695200 -1.37539300
H -6.74133200 2.82958700 -3.10415600
H -7.28646400 1.53428300 -2.03269000
C -5.89315400 -0.33058200 2.23048000
C -6.07711900 1.08363700 2.83133400
H -6.54551200 1.77113700 2.11806600
H -6.71930000 1.03913200 3.71940800
H -5.11369700 1.51108200 3.13250200
C -7.27726900 -0.90893400 1.84419100
H -7.17362700 -1.90240700 1.39282400
H -7.91258200 -1.00531900 2.73316600
H -7.80254300 -0.27006000 1.12634000
C -5.27905300 -1.23503600 3.31698000
H -4.29801400 -0.87486300 3.64609100
H -5.93775600 -1.25358300 4.19279700
H -5.16544600 -2.26791200 2.96862200
C -1.76744400 -2.88760300 -0.49316600
C -3.03043900 -3.69654300 -0.58699600
C -3.92843100 -3.53543200 -1.65172400
H -3.72868100 -2.79282700 -2.41702500
C -5.07011500 -4.33233600 -1.73374800
H -5.75413100 -4.20499100 -2.56824800
C -5.33439900 -5.28892900 -0.75083400
H -6.22858200 -5.90303300 -0.81423900

C -4.44278700 -5.45663700 0.31035400
H -4.64028400 -6.19962500 1.07829200
C -3.29023000 -4.67380900 0.38531400
H -2.59220500 -4.80746200 1.20730900
C -0.57262700 -3.66217000 -0.52049500
H -0.71053500 -4.71783800 -0.70772300
C 0.72899000 -3.19110000 -0.42414200
C 1.89088200 -4.11125200 -0.55318500
C 1.79221700 -5.48526800 -0.27295100
H 0.85968700 -5.90006900 0.09593200
C 2.89611000 -6.32022000 -0.42895500
H 2.80686600 -7.37830800 -0.19880500
C 4.11415500 -5.79870000 -0.87273300
H 4.97285300 -6.45251400 -0.99939500
C 4.22491800 -4.43315500 -1.14454500
H 5.16838900 -4.01952300 -1.48951900
C 3.12571400 -3.59251400 -0.97746500
H 3.20976900 -2.53125500 -1.18124900